OPEN ACCESS

Geology ARTICLE

Mid-Holocene rainfall heterogeneity in subtropical East Asia

Hai Xu,[1,2,*] Jian Cao,[3] Jing Wang,[1] Jun Cheng,[3] Yonaton Goldsmith,[4] and Hao Long[5]

*Correspondence: xuhai@tju.edu.cn

Received: January 20, 2026; Accepted: April 9, 2026; Published Online: April 13, 2026; https://doi.org/10.59717/j.xinn-geo.2026.100225

GRAPHICAL ABSTRACT

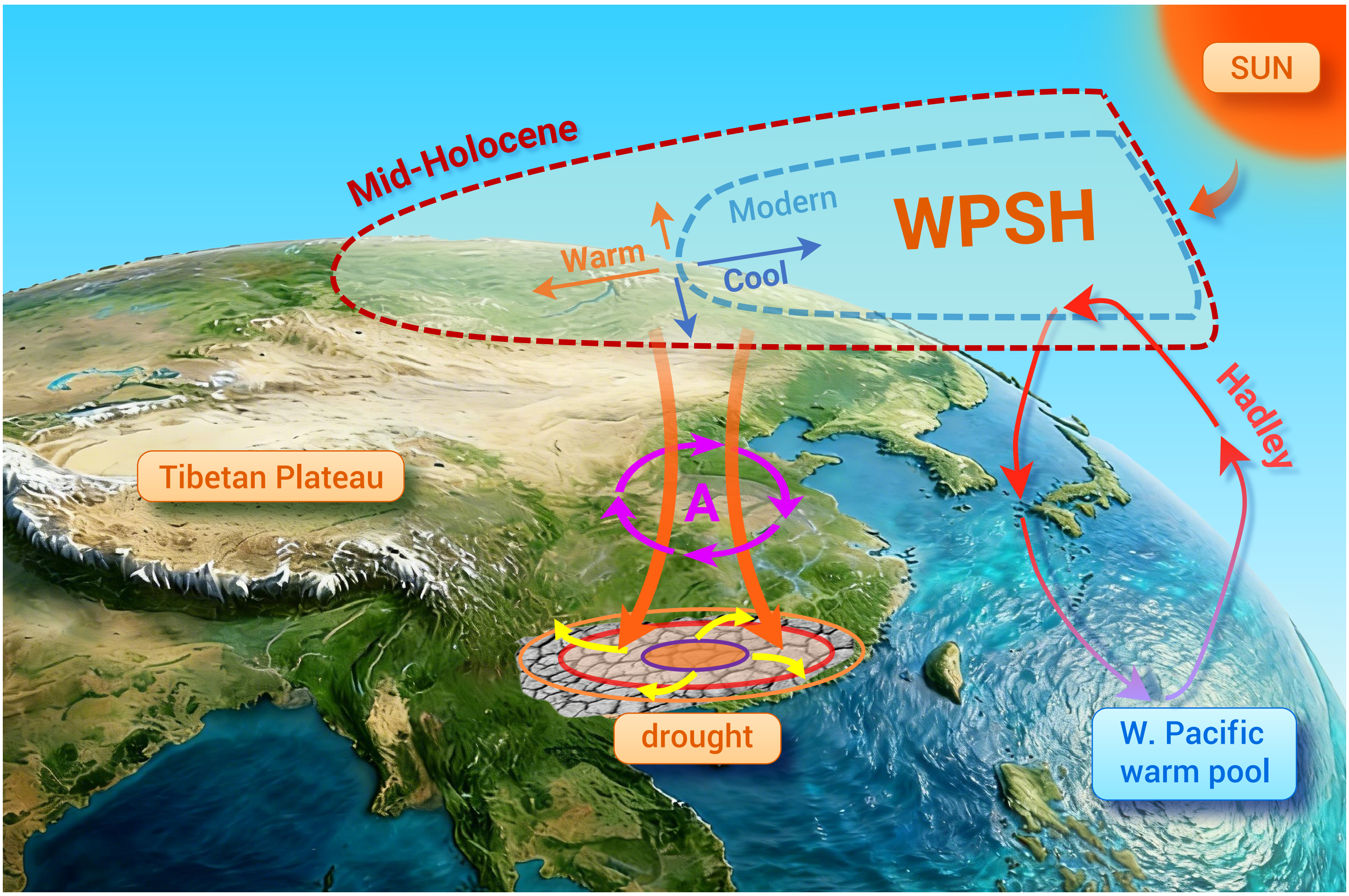

PUBLIC SUMMARY

- Western Pacific Subtropical High (WPSH) shapes the long-term rainfall heterogeneity in subtropical East Asia.
- Mid-Holocene warming intensified the WPSH and led to prolonged droughts in subtropical East Asia.
- Late Holocene cooling resulted in a weakened WPSH and increased precipitation in subtropical East Asia.
- Solar forcing and the related temperature gradients likely regulate the long-term WPSH behaviors.

Mid-Holocene rainfall heterogeneity in subtropical East Asia

Hai Xu,[1,2,*] Jian Cao,[3] Jing Wang,[1] Jun Cheng,[3] Yonatan Goldsmith,[4] and Hao Long[5]

[1]Key Laboratory of Karst Georesources and Environment, Ministry of Education, Guizhou University, Guiyang 550025, China
[2]Institute of Surface-Earth System Science, School of Earth System Science, Tianjin University, Tianjin 300072, China
[3]Nanjing University of Information Science and Technology, Nanjing 210044, China
[4]Institute of Earth Sciences, the Hebrew University of Jerusalem, Jerusalem 91904, Israel
[5]Nanjing Institute of Geography and Limnology, Chinese Academy of Sciences, Nanjing 211135, China
*Correspondence: xuhai@tju.edu.cn

Received: January 20, 2026; Accepted: April 9, 2026; Published Online: April 13, 2026; https://doi.org/10.59717/j.xinn-geo.2026.100225

Citation: Xu H., Cao J., Wang J., et al. (2026). Mid-Holocene rainfall heterogeneity in subtropical East Asia. *The Innovation Geoscience* **4**:100225.

Growing lines of evidence reveal an unexpectedly dry mid-Holocene but wetting late Holocene in subtropical East Asia, which is anti-phase/out-of-phase to the widely recognized northern hemisphere solar-insolation-forced Asia summer monsoon precipitation trend. This asynchrony implies that some key processes are missing in the current understanding of the Asia summer monsoon dynamics across different monsoon subsystems. Here we further confirm this spatial rainfall heterogeneity with robust biogeological evidence, corroborated by archeological evidence and simulations of transient climatic models. We propose that the location and intensity of the western Pacific subtropical high (WPSH) are most likely responsible for the observed orbital/suborbital spatial hydroclimatic heterogeneity, while the tropical Indo-Pacific sea surface temperature (SST), the SST gradients between the west-east equatorial Pacific, as well as the temperature gradients between southern-northern hemispheres, are the governing factors that combinedly regulate the WPSH behaviors and ultimately modulate the orbital/suborbital rainfall heterogeneity in subtropical East Asia.

INTRODUCTION

Globally, areas controlled by subtropical highs are generally characterized by higher temperatures and less precipitation due to the anticyclone feature of the subtropical highs, which is responsible for the widely distributed arid/semi-arid landscapes in the global subtropical zones.[1] The uplift of the Tibetan Plateau has intensified Asia summer monsoon (ASM) and the associated water vapor transportation,[2-4] triggering a transition from arid/desert to wet conditions in subtropical East Asia since the early Neogene,[1] and resulting in the modern "South Yangtze River water towns" that are obviously different to the widely distributed arid/semi-arid landscapes in the global subtropical zones. Thus, rainfall patterns in subtropical East Asia are the result of competing processes: the drying effect of the subtropical highs and the rainfall effect of the ASM, which might operate differently on different timescales.

On seasonal/annual scales, the WPSH significantly influences the modern rainfall distribution in subtropical East Asia. One example should be the year 2022, when the WPSH was unprecedently strong and extended westward to approximately 90°E, leading to serious summer/autumn rainfall failure and a once-a-century drought across the entire Yangtze River reaches;[5] both the riverine runoff and sand loads were also significantly decreased.[6] On decadal/centennial scales, the movement and changes in intensity of the WPSH can largely influence the rainfall differences between its core zone and the south and north China, leading to clearly spatiotemporal rainfall heterogeneity, such as the tripolar and bipolar rainfall patterns, which have been observed both in the modern epoch and in the last millennium.[7,8]

On orbital/suborbital scales, classical Asia monsoon forcing theory holds that Northern Hemisphere summer solar insolation governs the intensity of the Asian summer monsoon.[9,10] Therefore, it has long been widely accepted that the long-term trends of monsoon precipitation are consistent across the East Asian Summer Monsoon domain, the Indian Summer Monsoon domain, and their transitional zones. Whereas, the recent one more decade saw increasing lines of biogeological evidence pointing to heterogenous rainfall patterns in subtropical East Asia, i.e., relatively dry mid-Holocene but wetting late Holocene in subtropical East Asia,[11,12] which is clearly anti-phase/out-of-phase to the trends of NH summer solar insolation,[13] north China precipitation,[14] as well as the stalagmite-$\delta^{18}O$-based ASM intensity.[15] Thus, there is a need to reconstruct and confirm the spatiotemporal characteristics of the heterogenous rainfall patterns on orbital/suborbital timescales and understand the mechanisms that govern these processes.

Subtropical East Asia is defined here as roughly (but not necessarily limited to) the region between (90°E-140°E, 15°N-35°N; Figure 1); this area is densely populated and is one of the main regions of the global early civilizations. Knowledge of the spatiotemporal rainfall heterogeneity and its linkage to the long-term WPSH behavior is critical not only for a more comprehensive understanding of the ASM dynamics, but also for understanding the relationship between natural hydroclimatic changes and early civilization development. In this study, we developed a new record and compiled robust paleoclimate records from this region (Figure 1 & Table S1). We focus on the orbital/suborbital rainfall heterogeneity inferred from these lines of biogeological evidence, and compared it with archeological evidence and transient climate simulations; the forcing mechanisms of the observed rainfall heterogeneity were then particularly discussed.

MATERIALS AND METHODS

Lake Caohai records

We collected a surface short core (CH18-3-4; 137cm long) in the deep central area of Lake Caohai, 2018, and sampled the core at an interval of every 1 cm. Radioactivity of ^{137}Cs and ^{210}Pb was measured by a gamma detector (Ortec Germanium (HPGe) well detector; GWL-15-250; Figure 2). Twenty-two samples were dated by radiocarbon dating (Figures 3-4, Text S1 & Table S2). Element compositions were determined on an X-ray fluorescence spectrometry (Bruker S8 Tiger series II). In this study, the sedimentary Fe/Mn and Sr/Ca ratios were used to trace the long-term weathering intensity (see details in Text S2), lower sedimentary Fe/Mn and Sr/Ca ratios corresponding to stronger chemical weathering and higher rainfall amount, and vice versa, which is consistent with the long-term monsoon precipitation as inferred from other proxy indices (see Figures 5 & S1).

Other data collection

Lake Xingyun radiocarbon reservoir. We corrected the radiocarbon ages in Lake Xingyun[18] by subtracting an old carbon reservoir of ~250 years based on the radiocarbon dating of the modern lake water, living submerged waterweeds, and living aquatic snails (see details in Table S3).

Lake Huguangyan. Sedimentary total organic carbon flux in Lake Huguangyan is calculated based on the total organic carbon content (TOC) and bio-SiO_2 contents and the bio-SiO_2 flux data provided in Yancheva et al., 2007,[19] using an equation: $Flux_{TOC} = Flux_{bio\text{-}Sio2} * [TOC]/[bio\text{-}SiO_2]$. We do not use the TOC flux data of the last 2000 years to avoid possible strong anthropogenic impacts.

Data assimilation. We normalized curves compiled in this study (Figures 5e-p) to [-1,1] and then resampled each curve with a common 10-yr resolution. The resampled data were then stacked to generate a composited one (Figure 5q), and was used to represent precipitation over the subtropical East Asia areas.

Climatic parameter definition

The WPSH intensity, WPSH ridge line, and the WPSH western ridge point are defined below:

The WPSH ridge line index is characterized by the mean of the latitude location of the zonal wind shear line where the zonal wind u = 0 and ∂u/∂y > 0 encircled by the 5880 gpm isolines within the range of 110°E-150°E and north

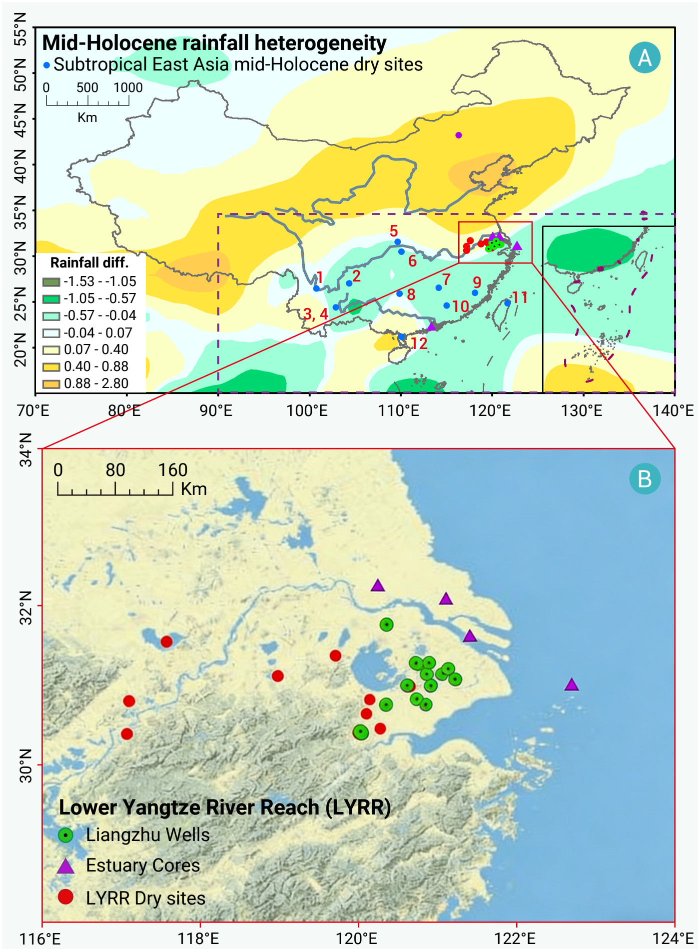

Figure 1. Mid-Holocene rainfall heterogeneity in subtropical East Asia (A) shows the compiled mid-Holocene dry sites in subtropical East Asia (purple rectangle; 90°E-140°E, 15°N-35°N). Orange-cyan shades show summer (June to September) rainfall difference between mid-Holocene (8000-6000 a BP) and 4200 a BP based on TraCE simulation (mm/day; orange and cyan correspond to a wetter mid-Holocene and a wetter later Holocene, respectively).[16] (B) is a magnified view of the red rectangle in A and shows the mid-Holocene dry sites in the lower Yangtze River reach (LYRR) inferred from sedimentation rates and archaeological evidence. Blue filled circles with red digital numbers in (A) denote parts of the mid-Holocene dry sites mentioned in the text (see details in Table S1). Red filled circles (both in A & B) show lakes and wetlands that exhibited a drop in sedimentation rate during ~7000-4000 a BP; while green circles show the locations of the Liangzhu ancient wells (note some of the points are overlapped).[17] Purple triangles show the riverine estuary areas where the sedimentation rates were dropped during the mid-Holocene (Table S1). Purple filled circle in panel A shows the location of Lake Dali in northern China, of which the lake-level changes are thought to represent the history of northern China precipitation.[14]

of 10°N; If there is no 5880 gpm isoline, the zonal wind shear line ($u = 0$ and $\partial u/\partial y > 0$) encircled by the 5840 gpm isolines will be considered. If the 5840 gpm isolines are absent, the historical minimum value of the corresponding month since 1951 will be taken as the substitute.

The WPSH western ridge point is the westernmost point characterized by the longitude of the westernmost 5880 gpm isolines within the range of 90°E-180°E and north of 10°N. If it lies to the west of 90°E, it will be denoted uniformly as 90°E; if there is no 5880 gpm isoline in a certain month, the historical maximum value of the corresponding month since 1951 will be taken as the substitute.

RESULTS

Age model of Core CH18-3-4

A ^{137}Cs peak was observed at 22cm in Core CH18-3-4 (Figure 2A), corresponding to the 1964-yr time-marker.[20,21] Global multi-national above-ground nuclear weapon tests began in the early 1950s, and atmospheric ^{137}Cs fallout can be detected in lake sediments from approximately AD 1952.[20,21] As shown in Figure 2A, the ^{137}Cs departures from baseline at 25cm, which can be used as the time-marker of AD 1952. The ^{210}Pb activity show a broadly exponential

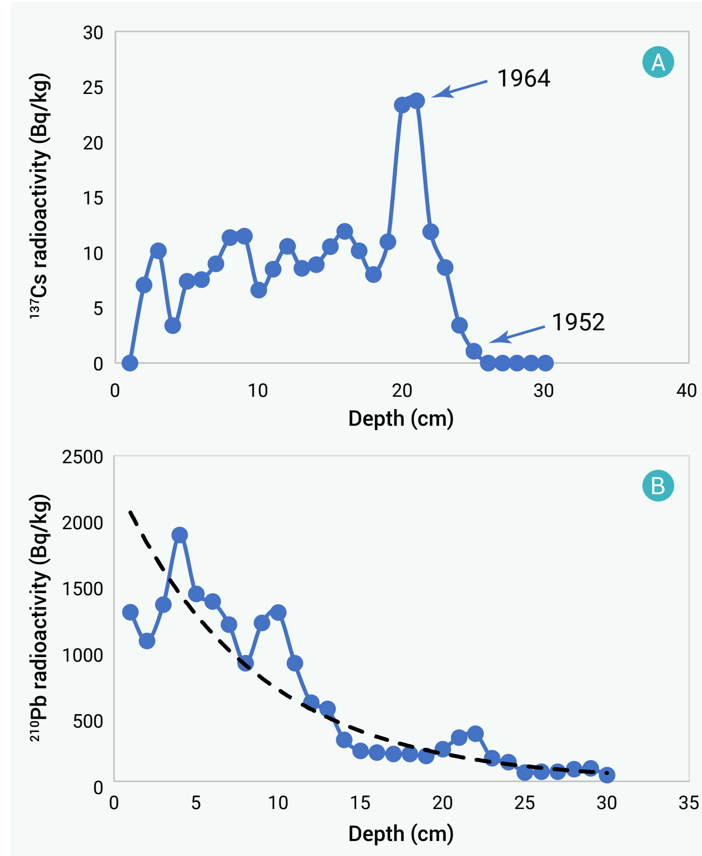

Figure 2. Radioactivity of ^{137}Cs (A) and ^{210}Pb (B) in Core CH18-3-4 in Lake Caohai Two time-markers of 1964 and 1952 are identified according to the ^{137}Cs radioactivity (A); dotted curve in (B) is the logarithmic fit of the ^{210}Pb radioactivity.

pattern (Figure 2B), suggesting a stable sedimentation process at the deep-central area in Lake Caohai during the past several decades.[21] The fraction modern carbon (F^{14}C) values of two samples (CH18-3-4-20 and CH18-3-4-10) are 1.06778 and 1.28369, respectively, suggesting that these two samples are modern samples. The ^{14}C ages of these two modern samples were obtained by comparing with the modern global atmospheric ^{14}C concentration curve (Figure 3; http://calib.org/CALIBomb/), which are consistent with the results inferred from the ^{137}Cs age model.

An old carbon reservoir of 604 years was estimated by comparison between the ^{14}C ages and the ^{137}Cs time-markers. Both a linear age model and a bacon age model were generated based on the corrected ^{14}C ages and the ^{137}Cs timer-markers (Figure 4), and the results are similar; we used the bacon age model in this study. The lithological facies and the ^{14}C ages suggest that a hiatus could have occurred between the last glaciation maximum and the Holocene (Figure 4); while from the early Holocene to mid-Holocene, Lake Caohai was most likely a shallow wetland and/or almost desiccated, with a low sedimentation rate as compared to the late Holocene (Text S1).

Biogeological evidence for the orbital/suborbital rainfall heterogeneity

Southwest China. We previously reconstructed lake level changes of Lake Chenghai, a closed-basin lake in southwestern China with robust beach-evidence (Figure 5e),[12] and the results show that from the last deglaciation to the early Holocene (~16000-8000 a BP) lake levels were similar in trends to the stalagmite δ^{18}O in Dongge Cave (Figure 5b),[15] the sedimentary records at Lake Tengchong-Qinghai[22] and Lake Huguangyan,[19] as well as the reconstructed lake levels at Lake Dali (Figure 5c).[14] However, Lake Chenghai experienced a low lake level period during the mid-Holocene (~8000-4000 a BP), while during the late Holocene (~4000 to 100 a BP) the lake levels were gradually arising (Figure 5e), indicating a prolonged drought during the mid-Holocene but wetting trend during the late Holocene, which is inverse to the widely recognized NH summer solar insolation trend (Figure 5a),[13] the stalagmite δ^{18}O-based ASM trend (Figure 5b),[15] and the lake level-based north

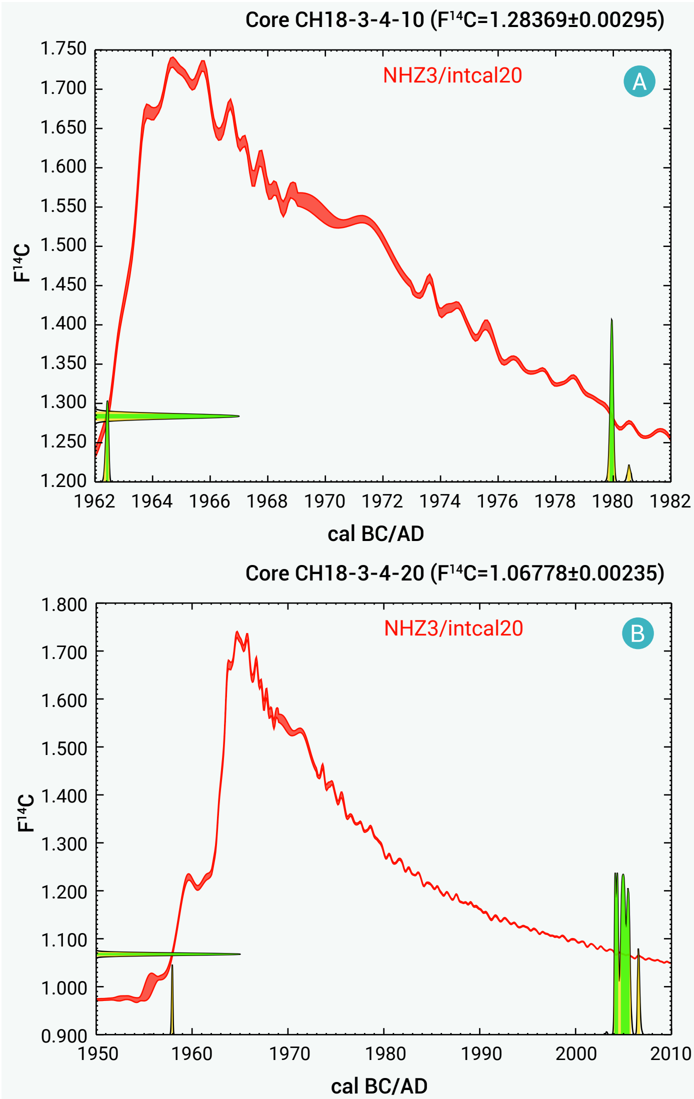

Figure 3. The fraction modern carbon ($F^{14}C$) of two surface samples (CH18-3-4-10:1979AD, left; CH18-3-4-20:1958AD, right) in Core CH18-3-4 in Lake Caohai The ^{14}C ages were obtained by comparing with the global atmospheric ^{14}C concentration curve (http://calib.org/CALIBomb/).

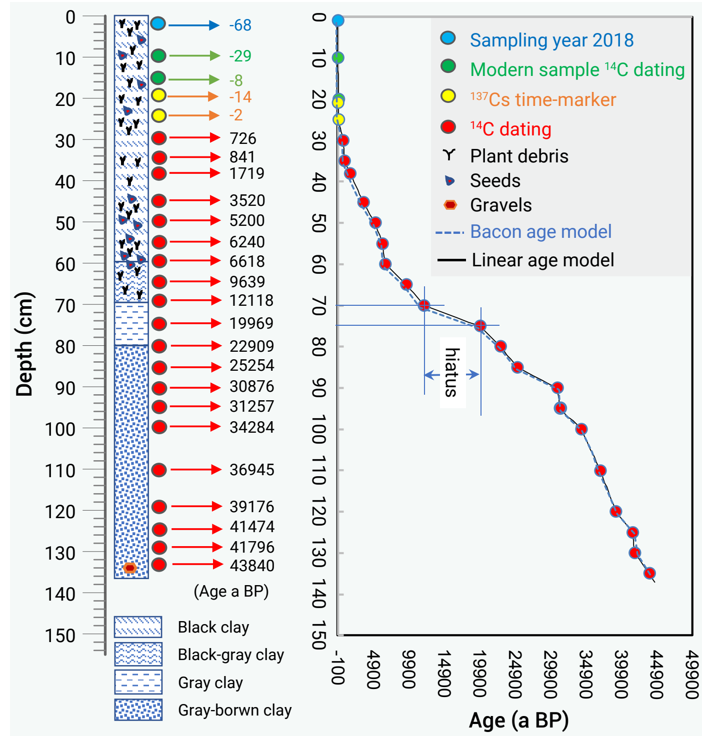

Figure 4. Age model of Core CH18-3-4 in Lake Caohai.

China precipitation trend (Figure 5c).[14]

The age model of Core CH18-3-4 in Lake Caohai (Figure 4, see more details in Text S1) and changes in lithological facies suggested that the lake was almost desiccated during the mid-Holocene and expanded during the late Holocene, consistent with the lake level changes in Lake Chenghai.[12] The sedimentary Fe/Mn (Figure 5d) and Sr/Ca ratios (Figure S1) in Lake Caohai suggest weak chemical weathering and low precipitation during the mid-Holocene, but stronger chemical weathering and higher precipitation during the late Holocene (Text S2), which is also consistent with the lake level changes at Lake Chenghai (Figure 5e).

The sedimentary carbonate contents in Lake Xingyun[18] and Lake Fuxian[23] were increased since the early Holocene and reached the highest values at approximately 3000 a BP (as high as ~50%); after 3000 a BP, they gradually decreased to the recent content (~10%) (Figures 5g-h). Such high carbonate contents during the mid-Holocene in both lakes point to substantial chemical precipitation due to high lake water salinities, which is likely due to the contemporarily relatively lower rainfall amount and stronger evaporation during the mid-Holocene. This is consistent with the rainfall trends inferred from the lake levels at Lake Chenghai[12] and the Fe/Mn ratios in Lake Caohai (Figure 5).

Middle Yangtze River reach and adjacent regions. Hopanoid concentration increased significantly in the Dajiuhu peatland (Figure 5h), middle Yangtze River reach during the mid-Holocene,[11] suggesting a lowered peatland water table and decreased precipitation. The hopanoid concentration in Zhaogongting peatland in Yanling County, Hunan Province, shows similar trend (Figure 5i).[24] The peatland water table quantitatively reconstructed from fossil phytoliths also shows a relatively dry period between 7500-3500a BP at Dajiuhu peatland, and the peat deposition rate dropped sharply and even stopped.[25] The magnetic parameters in stalagmites in this region also suggest an increasing precipitation trend from mid-Holocene to late Holocene (Figure 5j).[26] TOC values in the Daping peatland were low during the mid-Holocene but showed an increasing trend during the late Holocene,[27] also suggesting a "dry mid-Holocene but wetting late Holocene" (Figure 5m). These lines of evidence suggest drought conditions over the middle Yangtze River reach and adjacent regions during the mid-Holocene.

Lower Yangtze River reach and adjacent regions. Sedimentation rates in many lakes/wetlands in the lower Yangtze River reach slowed down substantially and even stopped during the period of ~7000-4000 a BP. This phenomenon has been observed in Nanyi Lake, Caizi Lake, Shengjin Lake,[28] as well as in a large number of wetlands in the Hangjiahu Plain (see locations in Figure 1),[29-31] indicating widely extended drought conditions over the lower Yangtze River reach. One example is the Dongtiaoxi River, where sedimentation rate declined and the river channel was replaced by peatland during the period of ~7000-4000 a BP,[29] suggesting a desiccated or shallow wetland environment. Chemical weathering indices of Nanyi Lake (Figure 5p) also point to relatively weak precipitation during the mid-Holocene.[32] Collectively, these lines of evidence suggest a broad range of drought in the lower Yangtze River reach during the mid-Holocene.

Southeast coast zone. The sedimentary Ti contents in Lake Huguangyan are similar in trend to the hydroclimatic trends inferred from other indices, such as lake levels in Lake Chenghai from the last deglaciation to mid-Holocene (Figure 5k);[12,19] while during the late Holocene the sedimentation rates increased by 2-3 times due to enhanced human activities around Lake Huguangyan, which could have diluted the Ti content and masked the climatic significance.[12,19] Whereas the calculated sedimentary TOC flux in this lake (Figure 5l; see MATERIALS AND METHODS) also points to a relatively dry mid-Holocene, similar to the precipitation trend in subtropical East Asia. The sedimentary Fe/Mn and Rb/Sr ratios of Lake Huguangyan also suggest a relatively dry mid-Holocene (see the Rb/Sr ratios in Figure 5n as an example).[33] In addition, the K/Rb ratios in Dahu Lake, north Taiwan, indicate enhanced weathering and increased runoff and precipitation during the late Holocene (Figure 5o).[34] The lithological facies of a sediment core in Lake Dahu, Jiangxi Province, southern China, indicate that the lake shifted from

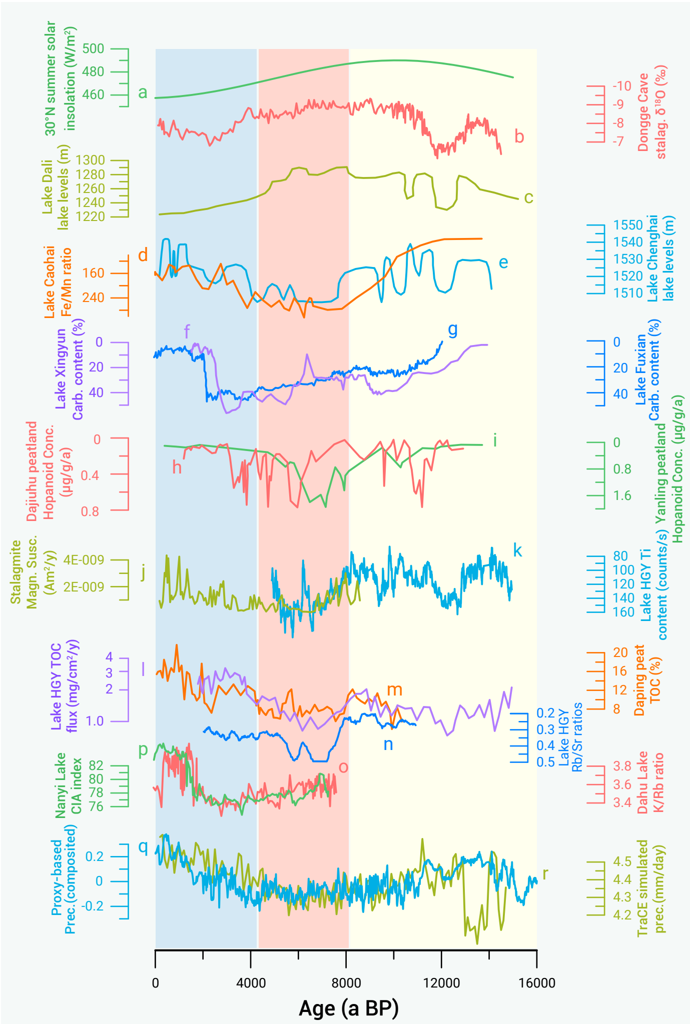

Figure 5. Comparison between hydroclimates in subtropical East Asia, NH summer solar insolation (curve a),[13] and ASM precipitation inferred from stalagmite δ^{18}O (curve b)[15] c. Lake levels of Lake Dali.[14] d. Sedimentary Fe/Mn ratios in Lake Caohai (this study). e. Lake levels of Lake Chenghai.[12] f. Sedimentary carbonate content in Lake Xingyun (see MATERIALS AND METHODS).[18] g. Carbonate content in Lake Fuxian.[23] h. Hopanoid concentration in Dajiuhu peatland, Hubei Province.[11] i. Hopanoid concentration in Zhaogongting peatland, Yanling County, Hunan Province.[24] j. Stalagmite magnetic susceptibility in Heshang Cave, Hubei Province.[26] k. Sedimentary Ti content in Lake Hguangyan.[19] l. Total organic carbon flux in Lake Huguangyan (see MATERIALS AND METHODS).[19] m. TOC content in Daping peatland, Hunan Province.[27] n. sedimentary Fe/Mn ratios in Lake Huguangyan.[33] o. K/Rb ratio in Lake Dahu, north Taiwan.[34] p. Chemical weathering index (CIA) in Lake Nanyi.[32] q. Composited subtropical East Asia precipitation (based on indices from e to p; see MATERIALS AND METHODS). r. Simulated precipitation in TraCE-21ka simulation in subtropical East Asia (20°N-27°N; 110°E-125°E).[12,16] Vertical red rectangle shade represents the mid-Holocene. See details in Table S1.

lake to peatland during ~6000-4000 a BP, and shifted from peatland to lake again after ~4000 a BP, which also points to a dry mid-Holocene and wetting late Holocene.[35,36] The peat cellulose δ^{18}O from a peatland in Fujian Province, southeastern China,[37] also indicates an increasing precipitation trend from the middle to late Holocene.

Estuary sedimentation rate. Sedimentation rates of several cores collected in the Yangtze River estuary (see locations in Figure 1 & Table S1) were much lower during the period of ~7000-4000 a BP, suggesting less sand load, which should be most-likely ascribed to the decreased runoff, and averagely reduced precipitation in the Yangtze River reach during this period. This is analogous to the modern observed "decreased precipitation~decreased sand load" relationship across the entire Yangtze River reach, e.g., in 2022,[6] and is consistent with the aforementioned lines of biogeological evidence that point to a drought mid-Holocene. In addition, the sedimentation rates at the Pearl River estuary were also lower during the mid-Holocene.[38] Based on records compiled above, we contend that the mid-Holocene drought can be extended to a wide region in subtropical East Asia (including both the Yangtze River reach and the Pearl River reach). We previously extracted precipitation in the subtropical East Asia (20°N-27°N; 110°E-125°E; Figure 5r) from TraCE simulation,[12,16] and the result is also similar in trends to the precipitation inferred from the above-mentioned evidence in subtropical East Asia (see each curve and a composited one in Figure 5).

Evidence from the development of early Chinese civilization

Subtropical East Asia is densely populated and thus the mid-Holocene drought could have impacted the development of the early Chinese civilization in this region. Due to the primitive techniques, early ancestors generally settled in warm and arid regions close to water. For example, the Mesopotamian Civilization, the Egyptian Civilization, and the Indus River Civilization, all thrived in warm arid environments and were adjacent to big rivers.[39] The archaeological sites of the mid-Holocene in subtropical East Asia, especially between 5300-4000 a BP, were centered in the lowland and streamsides in the Jianghan Basin, middle Yangtze River reach,[11] of which some ancient settlements are submerged today. This ancient settlement pattern suggests a relatively dry condition at that time. During the late Holocene, the archaeological sites are located in higher elevations, such as the archaeological sites of the Xia and Shang Dynasties during 4000-3000 a BP,[11] implying wetter conditions during this time. Such hydroclimatic conditions inferred from the distribution of archaeological sites are roughly consistent with those inferred from biogeological evidence, supporting a mid-Holocene drought on one hand, and providing clues to understand how early human societies adapted to nature on the other hand.

The Taihu Lake in the lower Yangtze River reach experienced a substantial contraction in the mid-Holocene,[40] and considerable remains of the Liangzhu Culture (5300-4000 a BP) are submerged in the modern lake (e.g., stone axe, stone port, triangle pottery, etc.),[40] suggesting dry conditions during the mid-Holocene that favored people settling around the lake's periphery. The lake was gradually filled during the late Holocene, as can be inferred from the Chunqiu wells (Chunqiu period: ~770BC-476BC) buried under the modern lake,[40] suggesting increased precipitation during the late Holocene. The Taihu Lake area was about 1680 km^2 in the East Han Dynasty as recorded in an ancient book of "Yue Jue Shu" (《越绝书》; written in East Han Dynasty about 2200 years ago), which is approximately 60% of the modern Taihu Lake,[40] suggesting increased precipitation around the Taihu Lake during the late Holocene. It is said that the Dayu Empire had managed floods around this area at the beginning of the Xia Dynasty (around 4100 a BP), which also implies increased precipitation at that time.[40]

The Dongtiaoxi River flows through the ancient Liangzhu city, and the Liangzhu Culture flourished during the period of ~5300-4300 a BP, suggesting a weak riverine runoff during this period. These results are consistent with the mid-Holocene droughts as inferred from the aforementioned biogeological evidence, and consistent with the sharp drops in sedimentation rates both in lakes and wetlands during this period.[29-31] A substantial portion (~77%) of the ancient wells in the lower Yangtze River reach belongs to the Liangzhu Culture (Figure 1),[17] and further subdivision shows that those ancient wells are mostly simple ash-pit type ancient wells (used for agricultural irrigation; "*Ancient Wells of the Liangzhu Culture*").[41] This may indicate that a widespread drought prevailed over the lower Yangtze River reach during this period and people had to rely on wells for their use and agriculture at that time. Moreover, underground water tables of the ancient wells in the Liangzhu Culture period were, in average, lower than those in the Songze Culture period (~5800-4900 a BP),[17] suggesting that the surface drought environment could have been more severe in the Liangzhu Culture period in this area. The recovery of the Dongtiaoxi River during ~4000-3000 a BP,[29] together with the above-mentioned late Holocene wetting evidence and the lack of foraminifera in the Liangzhu Culture layers,[17,42] suggests that the sudden abandonment of Liangzhu ancient city may be ascribed to strong floods caused by a sharp increase in precipitation at the beginning of the late Holocene. In summary, the aforementioned archaeological evidence supports a relatively dry mid-Holocene and wetting late Holocene in the lower Yangtze River reach.

DISCUSSION

Spatial rainfall heterogeneity over subtropical East Asia

The phenomenon of spatial differences in precipitation trends across different regions of monsoonal Asia has long been concerned. By comparing a vast number of proxy indices, An et al. suggested that precipitation changes across China exhibit pronounced regional differences, with precipitation peaks shifting from the Early Holocene in northern China to the Late Holocene in southern China.[43] The diverse responses of monsoon precipitation between different subsystems over monsoonal Asia during the Holocene, especially those between southern and norther China, have subsequently been extensively investigated through both climate simulations and biogeological approaches.[12,44-46] For example, by modeling and model-data comparing, Liu et al. showed an opposite precipitation trend between northern and southern China, with the precipitation in phase with summer insolation in northern China, but out of phase in southern China.[44] Based on comparison of biogeological records, Rao et al., can also show that Holocene humidity variations in the EASM region exhibit clear spatial differences: a humid mid-Holocene interval (ca. 8–3 ka BP) occurred in southern and northern China, but an arid interval from ca. 7–3 ka BP occurred in central China, especially in the middle reaches of the Yangtze River.[45] By comparing biogeological records from northern, central and southern China, as well as South Asia, with precipitation outputs simulated by a transient Earth system model, Ning et al., recently showed a mega - tripolar pattern of precipitation variations from the early to late Holocene over the entire ASM continental region, with precipitation peaked in the early Holocene over South Asia, northern and southern China, but in the late Holocene over central China.[46]

However, the mechanisms underlying the aforementioned spatial rainfall heterogeneity remain variable. An et al. proposed that the regional shift in the maximum precipitation belt from northwest to southeast over the past 10,000 years is a response to changing seasonality related to orbital forcing.[43] Chiang et al. ascribed the rainfall heterogeneity to the seasonal north-south movement of the westerly jet stream along the Tibetan Plateau,[47] which is closely related to north hemisphere solar insolation and North Atlantic climatic changes. Zhang et al. further confirmed the teleconnection between East Asia rainfall heterogeneity and the North Atlantic during the last deglaciation,[48] supporting the 'Jet Transition Hypothesis' discussed by Chiang.[47] They further suggested that a stronger meridional temperature gradient during stadial events and the resultant southward shifted and strengthened westerlies can lead to increased convection and uplift of moisture on the leeward side of the Tibetan Plateau during the summer months in central eastern China.[48] Liu et al. ascribed the observed rainfall differences between north and south China to changes in north hemisphere solar insolation and melting water in North Atlantic:[44] an increased insolation in summer leads to an increased land-sea temperature contrast, which enhances the WPSH, and then a wetter north China due to a stronger southerly wind over East China on the WPSH western flank; while on the other hand, a termination of the meltwater in the North Atlantic results in a northward migration of the ITCZ, a warmer Indian Ocean, an intensified WPSH, and eventually more rainfall in northern China (see details in ref.[44]).

Recent numerical simulations can even extend the spatial rainfall heterogenous pattern to several glacial-interglacial cycles.[49,50] For example, Dai et al., simulated the spatial rainfall heterogeneity using a fully coupled Earth System Model, and showed an inverse rainfall pattern in central-east China as compared to the north and south China, and such spatial rainfall heterogeneity can be extended to the past 425 ka.[49] They contended that the boreal summer insolation is the dominant forcing for the intensity of EASM and the response of WPSH is fundamental in modulating the precipitation pattern in monsoonal China on orbital timescales.[49] Wen et al., recently carried out a transient simulation forced by orbital parameters during the past 300 ka, and showed a grand dipole rainfall pattern between South Asia and Japan, with South China lying in a hybrid transition region.[50] They proposed that the dipole monsoon rainfall change between South Asia and Japan is related to the largescale circulation adjustment in response to northern hemisphere summer insolation.[50] However, although a large number of climate models are capable of reproducing the observed spatial rainfall heterogeneity over subtropical East Asia, some models still fail to do so,[51,52] indicating that uncertainties persist among different models and that the forcing mechanisms underlying the observed spatial rainfall heterogeneity require further investigation.

Influence of WPSH on spatial rainfall heterogeneity over subtropical East Asia

Changes in precipitation in East Asia are influenced by variable atmospheric circulations, including the WPSH, the El Niño -Southern Oscillation (ENSO), and the Pacific Decadal Oscillation (PDO), etc., and the spatiotemporal rainfall heterogeneity is most likely ascribed to the anticyclonic feature of the WPSH.[8,53] Changes in intensity and position of the WPSH on different timescales lead to the significant spatiotemporal rainfall difference between the core area and the surroundings (especially on the north and south sides of the WPSH), which constitutes a crucial physical prerequisite for the observed precipitation heterogeneity in East Asia;[8,49,53] while the influences of ENSO, PDO, etc., on the rainfall heterogeneity are thought to be mediated by the WPSH.[8] Therefore, one of the core tasks to study the rainfall heterogeneity in East Asia is to explore the WPSH behaviors on different timescales and its forcing mechanisms.

Seasonal/interannual scales. The WPSH core zone generally receive less precipitation due to the featured descending motion of the WPSH; while its edge areas receive more frontal precipitation due to strong airmass uprising occurs from the ascending motion.[8] The migration and changes in intensity of the WPSH lead to clear seasonal rainfall heterogeneity in the modern climate, like the well-known Meiyu rainy season generally in early-mid June and the hot-summer drought around Fujian Province generally in mid-July to mid-August, etc. Observations show that both the intensity and area of the WPSH increase from boreal spring to summer and decrease from autumn to winter.[54] The average WPSH ridge line advances northward in summer, and then withdraws to the south; while the WPSH western ridge extends westward and then withdraws to the east.[8,54] This seasonal march may imply that a warm climate state favors an intensifying and westwardly extension of the WPSH, consistent with the modern observations[54] and climatic simulations.[55]

The relationship between the WPSH and East Asia hydroclimates could be variable on short term timescales due to differences in both climates and local topography. The statistical analysis of the relationship between the WPSH ridge line and precipitation shows that a northwardly movement of the WPSH ridge generally corresponds to an intensified EASM, more summer precipitation in the north and northeast China but less in the "Yangtze-Huaihe River" areas;[56] meanwhile, a southward movement of the WPSH ridge line corresponds to a weakened EASM, less precipitation in north China but more in the "Yangtze-Huaihe River" areas.[56] Huang and Sun suggested that a higher SST in the western Pacific Warm Pool (WPWP) corresponds to an intensified convection around the Philippines to South China Sea and Sino-India Peninsula, favoring a northwardly advance of the WPSH, and more precipitation in the Huanghe River reach but less in the "Yangtze-Huaihe River" areas;[57] on the other hand, a cold SST in WPWP may lead to suppressed convection around the Philippines, a southwardly located WPSH ridge line, and less precipitation in the Huanghe River reach but more in the "Yangtze-Huaihe River" areas.[57]

Decadal/centennial scales. Modern observations also show significant bipolar or tripolar precipitation modes on decadal timescales in East Asia,[7] while high-resolution biogeological records show that such heterogeneous rainfall patterns also occurred during the last millennium.[8] This spatiotemporal rainfall heterogeneity has been linked to decadal/centennial movement and changes in intensity of the WPSH.[8] Model simulations show that the average ridge line of the WPSH coincides with precipitation in southern China and northern China: a northwardly located WPSH ridge line coincides with higher precipitation in south and north China but less in the central China, and vice versa (Figure S2).[8] While the decadal/centennial WPSH western ridge point is negatively correlated to precipitation in central China: a westwardly extended WPSH west ridge point corresponds to less precipitation over central China, and vice versa (Figure S2).[8]

The correlation analysis of the modern WPSH intensity and the Indo-Pacific SST shows that the SST of the warm pool is highly positively correlated to the WPSH intensity (R^2 = 0.50; see Figure S10B in ref.[8]): the higher SST, the stronger convective activity over the Indo-Pacific warm pool, the stronger Hadley circulation, and the stronger WPSH, and vice versa.[8,57] Modern observations also show that decadal higher SSTs over the Indo-Pacific warm pool generally coincide with stronger solar activity, suggesting a potential mechanism that can link the WPSH behavior with solar activity.[8,58] Such decadal/centennial relationships between solar activity, Pacific SSTs, and WPSH intensity can also be extended back to the last millennium (see Figures S2a-c & Table S4). We previously diagnosed the possible role of solar forcing by comparing the difference between high and low solar activity periods in the last millennium simulation from the ACCESS-ESM1-5 model (see

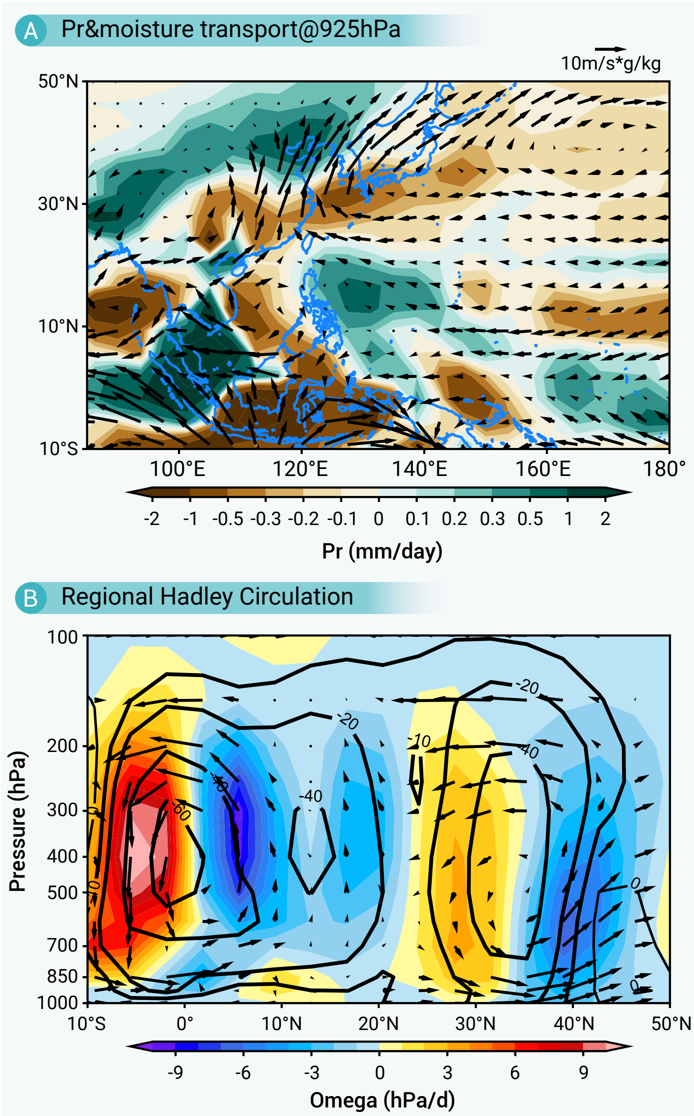

Figure 6. Differences in climate states between mid-Holocene (8000-6000 a BP) and 4200 a BP Panel a shows the averaged state of precipitation (brown-green shades; mm/day) and water vapor transport (arrows, m/s·g/kg^{-1}) based on TraCE21ka simulations.[16] Panel b shows the averaged regional Hadley circulation (over 100°E–140°E). The shades show differences in vertical pressure velocity (hPa·d^{-1}), arrows show the compositing of vertical pressure velocity (hPa·d^{-1}) and meridional wind (m·s^{-1}). Contours indicates the climatological vertical pressure velocity (hPa·d^{-1}). Negative values indicate ascending motion.

details in ref.[8]), and the results show that all of the SST, convection, cross-equatorial airflow, and the intensity of the Hadley circulation increase during strong solar activity. Under this scenario, the atmospheric circulations (e.g., ITCZ) shift northward, and the WPSH western ridge extends westward, resulting in more precipitation in north and south China but less in central China (the WPSH dominated core zone), leading to the observed decadal/centennial rainfall heterogeneity in subtropical East Asia.[8]

Orbital/suborbital scales. Our aforementioned compilations show a roughly bipolar pattern on orbital/suborbital scales, i.e., drier in north China and wetter in south China during the late Holocene, but wetter in north China and drier in south China during the mid-Holocene (Figure 1A). We contend that such orbital/suborbital spatiotemporal rainfall heterogeneity can also be ascribed to different WPSH behaviors. Multiple lines of evidence also show a wetting condition at ~4200 a BP in subtropical East Asia,[59,60] which contrasts to the dry conditions widespread over Asia-Africa monsoon areas (widely recognized as the 4200 a BP dry event); thus the 4200 a BP event can be regarded as a beginning of the late Holocene rainfall heterogeneity. To diagnose the rainfall differences between mid-Holocene and late Holocene, we evaluated the rainfall difference between 8000-6000 a BP and 4200 a BP in the TraCE21ka simulation (Figure 6a). The results show that over the monsoon frontier zone, during the mid-Holocene, the average monsoon precipitation was higher than during the late Holocene; while during the late Holocene the monsoon frontier zone shifted from wetter to drier but subtropical East Asia area shifted from drier to wetter. Thus, the TraCE21ka simulation shows similar results to those inferred from biogeological evidence (see locations in Figure 1).[61] The simulations in EC-Earth3-LR model also show a late Holocene wetting (as compared with the mid-Holocene; see Figure 6b in ref.[62]), consistent with the TraCE simulation and the biogeological evidence compiled in this study. As mentioned above, several other simulations can further extend the afore-mentioned rainfall heterogeneity across multiple glacial-interglacial cycles,[49,50] suggesting that the spatial precipitation heterogeneity during the mid-Holocene represents a natural phenomenon, rather than a result of human activities. In addition, the difference between 8000-6000 a BP to 4200 a BP shows that the 'mid-Holocene dry and late Holocene wetting' areas are roughly located over the tropical/subtropical oceans (see orange shades in Figure 6a), where only a small proportion is on land, including the subtropical East Asia. This may partly explain why late Holocene wetting biogeological evidence is sparse (as compared to the large number of mid-Holocene wetter evidence in the ASM marginal zone).

As shown in our diagnostics (Figure 6a), the difference between 8000-6000 a BP to 4200 a BP shows that the northward moisture transport in the lower troposphere is accelerated over eastern China, leading to moisture divergence and decreased precipitation in subtropical East Asia area. An abnormal water vapor convergence is evident over northern China, resulting in more precipitation and manifesting as a northward movement of the rainfall belt over East Asia. This northward migration of the rain belt is closely related to the northward extension of the Hadley cell. In boreal summer, the northern edge of the ascending branch of the regional Hadley circulation over East Asia is generally located between 30°N-40°N. While in our diagnostics, the ascending branch is located between 35°N-45°N (Figure 6b), which means the WPSH extended northward during the mid-Holocene (as compared with the 4200 a BP state; see causes below). These conditions are favorable for a northward migration of the rainfall belt, leading to a "south drought-north wet" hydroclimatic pattern during the mid-Holocene.

Possible forcing mechanism for the long-term WPSH behaviors

We examined the long-term behaviors of the WPSH in the TraCE simulations (see MATERIALS AND METHODS) and the results show that the WPSH gradually extended westward from the early Holocene, and reached the westernmost extent at about 4000-3000 a BP, and then gradually retreated eastward (as inferred from the WPSH western point; see Figure 7h). The average precipitation in subtropical East Asia extracted from TraCE simulation also shows a general dry mid-Holocene and a wetting late Holocene, broadly consistent with the WPSH western ridge extension and the hydroclimatic patterns inferred from the aforementioned biogeological evidence, suggesting a possible role of the WPSH in shaping the orbital/suborbital rainfall heterogeneity in subtropical East Asia (Figure 7).

Multiple factors could modulate the long-term WPSH behaviors, such as SSTs over the tropical Indo-Pacific and eastern tropical Pacific, and solar activity/insolation, etc.[8,44,53,55] For example, Liu et al. contended that the enhanced land-sea temperature contrast associated with variations in Northern Hemisphere summer solar insolation can intensify the intensity of the WPSH; meanwhile, changes in meltwater input to the North Atlantic can affect the surface thermal conditions of the Indian Ocean, which in turn excites an atmospheric Kelvin wave propagating toward the western Pacific and modulates the WPSH behaviors.[44] Piao et al. contended that the Green Sahara during the mid-Holocene would induce a westward shift of the Walker Circulation, which in turn would reduce rainfall over the western equatorial Pacific and intensify the WPSH via the Gill-Matsuno response; the westward shift of the Walker Circulation can also strengthen the Hadley Circulation, and ultimately result in an intensified and westward-shifted WPSH.[53] Dai et al., proposed that the northern hemisphere summer solar insolation plays a critical role in shaping the long-term behaviors of WPSH, which eventually modulates the central China rainfall heterogeneity.[49] We contend that the increased temperature during the mid-Holocene could have intensified the Hadley circulations during the boreal summer, and pushed the WPSH northward and westward, similar to the decadal/centennial scenarios where stronger solar activities lead to warmer SSTs and stronger Hadley circulations, and westwardly and northwardly extended WPSH.[8] The increased SSTs over tropical

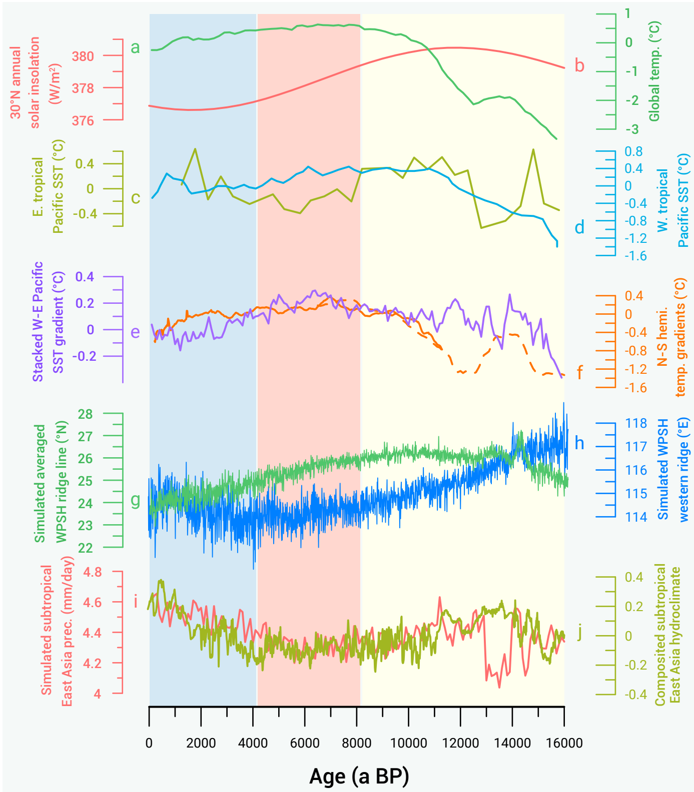

Figure 7. Comparison between orbital/suborbital WPSH behaviors, the hydroclimates in subtropical East Asia, and possible forcing a. Proxy-based global temperature variations.[65] b. NH 30° summer solar insolation.[13] c & d. SSTs in east and west tropical Pacific;[63] e. SST gradient between west and east tropical Pacific.[63] f. temperature gradient between south and north hemisphere ($\Delta T_{N\text{-}S}$).[66,67] g & h. Simulated WPSH ridge line and western ridge point in TraCE-21ka simulations.[12,16] i. Simulated precipitation in subtropical East Asia in TraCE-21kasimulations.[12,16] j. Composited proxy-based subtropical East Asia precipitation (see MATERIALS AND METHODS). Vertical red rectangle shade represents the mid-Holocene.

Indo-Pacific can also increase the tropical zonal SST gradient ($\Delta T_{W\text{-}E}$), strengthen the equatorial east wind, and eventually lead to a westward extension of the WPSH. As shown in Figure 7, the reconstructed $\Delta T_{W\text{-}E}$ was larger during the mid-Holocene,[63] which is favorable for a westward extension of the WPSH. Moreover, the mid-Holocene warmer conditions over north hemisphere could reduce the surface air pressure over the Tibetan Plateau, which is also favorable for a westward extension of the WPSH. The interhemispheric temperature gradient ($\Delta T_{N\text{-}S}$) could also influence the average location of the atmospheric convergence zone. It is suggested that a larger $\Delta T_{N\text{-}S}$ favors a northward advance of the ITCZ, NH subtropical highs (including the WPSH), and the NH westerly jet stream. In contrast, a smaller $\Delta T_{N\text{-}S}$ corresponds to southward movement of the above atmospheric circulations.[64] The simulated averaged WPSH ridge line is broadly in phase with the $\Delta T_{N\text{-}S}$ (Figures 7f-g), supporting the inferences above.

CONCLUSION

Increasing lines of biogeological evidence suggest a dry mid-Holocene but wetting late Holocene hydroclimatic trend in subtropical East Asia, which is anti-phase/out-of-phase to the NH summer solar insolation and ASM precipitation trends. Such an orbital/suborbital spatial rainfall heterogenous pattern is also supported by considerable archaeological evidence. We contend that the orbital/suborbital WPSH variability drives the observed rainfall heterogeneity. The SSTs over the tropical Indo-Pacific Oceans, the SST gradients between the west-east equatorial Pacific, as well as the temperature contrasts between south-north hemispheres, most likely dominate the long-term WPSH behaviors. If our hypothesis is correct, the role of the WPSH in regulating subtropical East Asian hydroclimates would strengthen under a continued warming scenario, which may lead to a reduction in water availability in subtropical East Asia and to a larger rainfall difference between monsoonal and subtropical East Asia.

REFERENCES

1. Guo Z. (2017). Loess Plateau attests to the onsets of monsoon and deserts (in Chinese). *Sci. China Earth Sci.* 47:421–437. DOI:10.1360/n072017-00037
2. Wu F., Fang X., Yang Y., et al. (2022). Reorganization of Asian climate in relation to Tibetan Plateau uplift. *Nat. Rev. Earth Environ.* 3:684–700. DOI:10.1038/s43017-022-00331-7
3. Ding L., Kapp P., Cai F., et al. (2022). Timing and mechanisms of Tibetan Plateau uplift. *Nat. Rev. Earth Environ.* 3:652–667. DOI:10.1038/s43017-022-00318-4
4. Guo Z. T., Ruddiman W. F., Hao Q. Z., et al. (2002). Onset of Asian desertification by 22 Myr ago inferred from loess deposits in China. *Nature* 416:159–163. DOI:10.1038/416159a
5. Hao L., Ma N. and He L. (2022). Circulation anomalies characteristics of the abnormal drought and high temperature event in the middle and lower reaches of the Yangtze River in summer of 2022 (in Chinese). *J. Arid Meteorol.* 40:721–732. DOI:10.11755/j.issn.1006-7639(2022)-05-0721
6. Zhang H., Cheng H., Sinha A., et al. (2021). Collapse of the Liangzhu and other Neolithic cultures in the lower Yangtze region in response to climate change. *Sci. Adv.* 7:eabi9275. DOI:10.1126/sciadv.abi9275
7. Ding Y., Wang Z. and Sun Y. (2008). Inter - decadal variation of the summer precipitation in East China and its association with decreasing Asian summer monsoon. *Part I: Observed evidences. Int. J. Climatol.* 28:1139–1161. DOI:10.1002/joc.1615
8. Xu H., Song Y., Cao J., et al. (2024). Heterogeneity of the East Asian rainfall influenced by solar-forced western Pacific subtropical high. *Commun. Earth Environ.* 5:1–9. DOI:10.1038/s43247-024-01660-9
9. Wang Y., Cheng H., Edwards R. L., et al. (2008). Millennial- and orbital-scale changes in the East Asian monsoon over the past 224,000 years. *Nature* 451:1090–1093. DOI:10.1038/nature06692
10. Hosner D., Wagner M., Tarasov P.E., et al. (2016). Spatiotemporal distribution patterns of archaeological sites in China during the Neolithic and Bronze Age: An overview. *Holocene* 26:1576–1593. DOI:10.1177/0959683616641743
11. Xie S., Evershed R.P., Huang X., et al. (2013). Concordant monsoon-driven postglacial hydrological changes in peat and stalagmite records and their impacts on prehistoric cultures in central China. *Geology* 41:827–830. DOI:10.1130/g34318.1
12. Xu H., Goldsmith Y., Lan J., et al. (2020). Juxtaposition of western Pacific subtropical high on Asian summer monsoon shapes subtropical East Asian precipitation. *Geophys Res Lett.* 47:e2019GL084705. DOI:10.1029/2019GL084705
13. Berger A. L. (1978). Long-term variations of caloric insolation resulting from the Earth's orbital elements. *Quat. Res.* 9:139–167. DOI:10.1016/0033-5894(78)90064-9
14. Goldsmith Y., Broecker W. S., Xu H., et al. (2017). Northward extent of East Asian monsoon covaries with intensity on orbital and millennial timescales. *Proc. Natl. Acad. Sci. USA* 114:1817–1821. DOI:10.1073/pnas.1616708114
15. Dykoski C. A., Edwards R. L., Cheng H., et al. (2005). A high-resolution, absolute-dated Holocene and deglacial Asian monsoon record from Dongge Cave, China. *Earth Planet. Sci. Lett.* 233:71–86. DOI:10.1016/j.epsl.2005.01.036
16. Liu Z., Otto-Bliesner B. L., He F., et al. (2009). Transient simulation of last deglaciation with a new mechanism for Bolling-Allerod warming. *Science* 325:310–314. DOI:10.1126/science.1171041
17. Zhu C., Wu L., Li L., et al. (2014). Research progress on Holocene environmental archaeology in the Yangtze River Valley, China. *Acta Geogr. Sin.* 69:1268–1283. DOI:10.11821/dlxb201409003
18. Wu D., Chen X., Lv F., et al. (2018). Decoupled early Holocene summer temperature and monsoon precipitation in southwest China. *Quat. Sci. Rev.* 193:54–67. DOI:10.1016/j.quascirev.2018.05.038
19. Yancheva G., Nowaczyk N. R., Mingram J., et al. (2007). Influence of the intertropical convergence zone on the East Asian monsoon. *Nature* 445:74–77. DOI:10.1038/nature05431
20. Lan J., Wang T., Chawchai S., et al. (2020). Time marker of ^{137}Cs fallout maximum in lake sediments of Northwest China. *Quat. Sci. Rev.* 241:106413. DOI:10.1016/j.quascirev.2020.106413
21. Xu H., Ai L., Tan L., et al. (2006). Geochronology of a surface core in the northern basin of Lake Qinghai: Evidence from ^{210}Pb and ^{137}Cs radionuclides. *Chin. J. Geochem.* 25:301–306. DOI:10.1007/s11631-006-0301-y
22. Zhang E., Zhao C., Xue B., et al. (2017). Millennial-scale hydroclimate variations in southwest China linked to tropical Indian Ocean since the Last Glacial Maximum. *Geology* 45:435–438. DOI:10.1130/g38309.1
23. Li T., Zhang H., Cai M., et al. (2019). The composition of carbonate matters in the sediments from Lake Fuxian and significance of paleoclimate and water level changes. *Quat. Sci.* 39:642–654. DOI:10.11928/j.issn.1001-7410.2019.3.11
24. Huang X., Zhang H., Griffiths M. L., et al. (2022). Holocene forcing of East Asian hydroclimate recorded in a subtropical peatland from southeastern China. *Clim. Dyn.* 60:981–993. DOI:10.1007/s00382-022-06333-x
25. Liu H., Gu Y., Huang X., et al. (2019). A 13,000-year peatland palaeohydrological response to the ENSO-related Asian monsoon precipitation changes in the middle Yangtze Valley. *Quat. Sci. Rev.* 212:80–91. DOI:10.1016/j.quascirev.2019.03.034
26. Zhu Z., Feinberg J. M., Xie S., et al. (2017). Holocene ENSO-related cyclic storms recorded by magnetic minerals in speleothems of central China. *Proc. Natl. Acad. Sci. USA* 114:852–857. DOI:10.1073/pnas.1610930114
27. Zhong W., Wei Z., Chen Y., et al. (2016). A 15.4-ka paleoclimate record inferred from δ^{13}C and δ^{15}N of organic matter in sediments from the sub-alpine Daping Swamp, western Nanling Mountains, South China. *J. Paleolimnol.* 57:127-139. DOI:10.1007/s10933-016-9935-x.

28. Yao S., Li C., Ling C., et al. (2019). About 3000 years of lake sediment hiatus due to relatively stable water level of the Yangtze River in the middle Holocene. *Quat. Sci.* 39:1148–1158. DOI:10.11928/j.issn.1001-7410.2019.05.07
29. Chen T., Ryves D. B., Wang Z., et al. (2018). Mid- to late Holocene geomorphological and hydrological changes in the south Taihu area of the Yangtze delta plain, China. *Palaeogeogr. Palaeoclimatol. Palaeoecol.* 498:127–142. DOI:10.1016/j.palaeo.2018.03.012
30. Liu Y., Sun Q., Thomas I., et al. (2015). Middle Holocene coastal environment and the rise of the Liangzhu City complex on the Yangtze delta, China. *Quat. Res.* 84:326–334. DOI:10.1016/j.yqres.2015.10.001
31. Ling G., Ma C., Yang Q., et al. (2021). Landscape evolution in the Liangzhu area since the early Holocene: A comprehensive sedimentological approach. *Palaeogeogr. Palaeoclimatol. Palaeoecol.* 562:110141. DOI:10.1016/j.palaeo.2020.110141
32. Liu J., Shen Z., Chen W., et al. (2021). Dipolar mode of precipitation changes between north China and the Yangtze River Valley existed over the entire Holocene: Evidence from the sediment record of Nanyi Lake. *Int. J. Climatol.* 41:1667–1681. DOI:10.1002/joc.6906
33. Wu X., Shen J. and Wang Y. (2011). The Holocene climate linkage between low latitude area and north Atlantic: Case study on element and element ratios of Huguangyan Maar lake. *Acta Sedimentol. Sin.* 29:926–934. http://www.cjxb.ac.cn/en/article/id/282
34. Chen H., Wen S., Song S., et al. (2012). Strengthening of paleo-typhoon and autumn rainfall in Taiwan corresponding to the Southern Oscillation at late Holocene. *J. Quat. Sci.* 27:964–972. DOI:10.1002/jqs.2590
35. Zhong W., Xue J., Cao J., et al. (2010). Bulk organic carbon isotopic record of lacustrine sediments in Dahu Swamp, eastern Nanling Mountains in South China: Implication for catchment environmental and climatic changes in the last 16,000 years. *J. Asian Earth Sci.* 38:162–169. DOI:10.1016/j.jseaes.2009.12.011
36. Zhou W., Yu X., Jull A. J. T., et al. (2004). High-resolution evidence from southern China of an early holocene optimum and a mid-holocene dry event during the past 18,000 Years. *Quat. Res.* 62:39–48. DOI:10.1016/j.yqres.2004.05.004
37. Song Y., Xu H., Lan J., et al. (2022). Enhanced human activity altered the late Holocene vegetation composition in subtropical East Asia. *Global Planet. Change* 214:103850. DOI:10.1016/j.gloplacha.2022.103850
38. Lin P., Xu X., Yan C., et al. (2022). Holocene sedimentary of the Pearl River Delta in South China: OSL and radiocarbon dating of cores from Zhuhai. *Front. Mar. Sci.* 9:1031456. DOI:10.3389/fmars.2022.1031456
39. Xia Z. (2012). Environmental Archaeology - Theory and Practice (in Chinese) (Peking University Press). DOI:10.4324/9780203784471
40. Zhang X. (2009). The course of the Taihu Lake's evolution in historical period (in Chinese). *J. Chin. Hist. Geogr.* 24:5–12. https://zgld.cbpt.cnki.net/portal/journal/portal/client/paper/1cbafbe5501284e57b2a84b45556da45
41. Ding J. (2015). Ancient wells of the Liangzhu culture (in Chinese) (Zhejiang Ancient Books Publishing House). https://www.lzmuseum.cn/WenHuaYanJiu/2019162158169.html
42. Zhu C., Song J., Long K., et al. (1996). Study on the Interruptions of the Shanghai Maqiao Culture (in Chinese). *Chin. Sci. Bull.* 41:148–152. DOI:10.1360/csb1996-41-2-148
43. An Z., Porter S. C., Kutzbach J. E., et al. (2000). Asynchronous Holocene optimum of the East Asian monsoon. *Quat. Sci. Rev.* 19:743–762. DOI:10.1016/s0277-3791(99)00031-1
44. Liu Z., Wen X., Brady E. C., et al. (2014). Chinese cave records and the East Asia Summer Monsoon. *Quat. Sci. Rev.* 83:115–128. DOI:10.1016/j.quascirev.2013.10.021
45. Rao Z., Li Y., Zhang J., et al. (2016). Investigating the long-term palaeoclimatic controls on the δD and $\delta^{18}O$ of precipitation during the Holocene in the Indian and East Asian monsoonal regions. *Earth-Sci. Rev.* 159:292–305. DOI:10.1016/j.earscirev.2016.06.007
46. Ning L., Xing F., Liu Z., et al. (2025). Mega - tripolar precipitation change accompanying water isotopes in Holocene Asian summer monsoon reanalysis. *Geophys. Res. Lett.* 52:e2025GL116451. DOI:10.1029/2025gl116451
47. Chiang J. C. H., Fung I. Y., Wu C.-H., et al. (2015). Role of seasonal transitions and westerly jets in East Asian paleoclimate. *Quat. Sci. Rev.* 108:111–129. DOI:10.1016/j.quascirev.2014.11.009
48. Zhang H., Griffiths M. L., Chiang J. C. H., et al. (2018). East Asian hydroclimate modulated by the position of the westerlies during Termination Ⅰ. *Science* 362:580–583. DOI:10.1126/science.aat9393
49. Dai G., Zhang Z., Otterå O. H., et al. (2021). A modeling study of the tripole pattern of East China precipitation over the past 425 ka. *J. Geophys. Res. Atmos.* 126:e2020JD033513. DOI:10.1029/2020jd033513
50. Wen Q., Liu Z., Jing Z., et al. (2024). Grand dipole response of Asian summer monsoon to orbital forcing. *npj Clim. Atmos. Sci.* 7:202. DOI:10.1038/s41612-024-00749-4
51. Sun Y., Wu H., Ramstein G., et al. (2023). Revisiting the physical mechanisms of East Asian summer monsoon precipitation changes during the mid-Holocene: A data–model comparison. *Clim. Dyn.* 60:1009–1022. DOI:10.1007/s00382-022-06359-1
52. Wu Y., Liu Y., Zhou W., et al. (2022). The mid-Holocene East Asian summer monsoon simulated by PMIP4-CMIP6 and PMIP3-CMIP5: Model uncertainty and its possible sources. *Global Planet. Change* 219:103986. DOI:10.1016/j.gloplacha.2022.103986
53. Piao J., Chen W., Wang L., et al. (2020). Northward extension of the East Asian summer monsoon during the mid-Holocene. *Global Planet. Change* 184:103046. DOI:10.1016/j.gloplacha.2019.103046
54. Liu Y., Ding Y., Gao H., et al. (2013). Tropospheric biennial oscillation of the western Pacific subtropical high and its relationships with the tropical SST and atmospheric circulation anomalies. *Chin. Sci. Bull.* 58:3664–3672. DOI:10.1007/s11434-013-5854-7
55. Zhou T., Yu R., Zhang J., et al. (2009). Why the Western Pacific subtropical high has extended westward since the late 1970s. *J. Clim.* 22:2199–2215. DOI:10.1175/2008JCLI2527.1
56. Zhang Q. and Tao S. (2003). The anomalous subtropical anticyclone in Western Pacific and their association with circulation over East Asia during summer (in Chinese). *Chin. J. Atmos. Sci.* 27:369–380. DOI:10.3878/j.issn.1006-9895.2003.03.07
57. Huang R. and Sun F. (1994). Impacts of the thermal state and the convective activities in the tropical western warm pool on the summer climate anomalies in East Asia. *Sci. Atmos. Sin.* 18:141–151. DOI:10.3878/j.issn.1006-9895.1994.02.02
58. Jin C., Liu J., Wang B., et al. (2019). Decadal variations of the East Asian summer monsoon forced by the 11-year insolation cycle. *J. Clim.* 32:2735–2745. DOI:10.1175/JCLI-D-18-0288.1
59. Zhang H., Cheng H., Cai Y., et al. (2018). Hydroclimatic variations in southeastern China during the 4.2 ka event reflected by stalagmite records. *Clim. Past* 14:1805-1817. DOI:10.5194/cp-14-1805-2018
60. Wang T., Li D., Cheng X., et al. (2022). Hydroclimatic changes in south-central China during the 4.2 ka event and their potential impacts on the development of Neolithic culture. *Quat. Res.* 109:39-52. DOI:10.1017/qua.2022.11
61. Goldsmith Y., Xu H., Torfstein A., et al. (2022). Abrupt contraction of the Indo - East Asian monsoons ended the Holocene humid period. *Geophys. Res. Lett.* 49:e2022GL100137. DOI:10.1029/2022gl100137
62. Zhang Q., Berntell E., Axelsson J., et al. (2021). Simulating the mid-Holocene, last interglacial and mid-Pliocene climate with EC-Earth3-LR. *Geosci. Model Dev.* 14:1147–1169. DOI:10.5194/gmd-14-1147-2021
63. Koutavas A. and Joanides S. (2012). El Niño-Southern Oscillation extrema in the Holocene and Last Glacial Maximum. *Paleoceanography* 27:PA4208. DOI:10.1029/2012PA002378
64. McGee D., Donohoe A., Marshall J., et al. (2014). Changes in ITCZ location and cross-equatorial heat transport at the Last Glacial Maximum, Heinrich Stadial 1, and the mid-Holocene. *Earth Planet. Sci. Lett.* 390:69–79. DOI:10.1016/j.epsl.2013.12.043
65. Osman M. B., Tierney J. E., Zhu J., et al. (2021). Globally resolved surface temperatures since the Last Glacial Maximum. *Nature* 599:239–244. DOI:10.1038/s41586-021-03984-4
66. Shakun J. D., Clark P. U., He F., et al. (2012). Global warming preceded by increasing carbon dioxide concentrations during the last deglaciation. *Nature* 484:49–54. DOI:10.1038/nature10915
67. Marcott S. A., Shakun J. D., Clark P. U., et al. (2013). A reconstruction of regional and global temperature for the past 11,300 years. *Science* 339:1198–1201. DOI:10.1126/science.1228026

FUNDING AND ACKNOWLEDGMENTS

This work was supported by the National Natural Science Foundation of China (Grant No.: 42361144842; U20A2078), the Leading Talent Project of Guizhou Province (BQW[2025]001), and the Natural Science Foundation of Jiangsu Province (BK20220108). The funders had no role in study design, data collection and analysis,decision to publish, or preparation of the manuscript.

AUTHOR CONTRIBUTIONS

H. Xu designed this study, analyzed the data, and wrote the paper. **J. Cao** and **J. Cheng** carried out climate simulations. **J. Wang** carried out data assimilations, **H. Long and Y. Goldsmith** discussed the climatic forcing mechanisms. All authors contributed to the manuscript and approved the final version.

DECLARATION OF INTERESTS

Hao Long is an Editorial Board member of The Innovation Geoscience and was blinded from reviewing or making final decisions on the manuscript. Peer review was handled independently of this member and their research group. The other authors declare no conflicts of interest.

DATA AND CODE AVAILABILITY

Data developed in this study are available on East Asian Paleoenvironmental Science Database:http://paleodata.ieecas.cn/FrmDataInfo_EN.aspx?id=42f4ca3b-8203-450c-b7e3-74cd4d6b8b0f.

SUPPLEMENTAL INFORMATION

It can be found online at https://doi.org/10.59717/j.xinn-geo.2026.100225.